Opportunistic Fluid Antenna Multiple Access

Kai-Kit Wong, *Fellow, IEEE,* Kin-Fai Tong, *Fellow, IEEE,* Yu Chen, *Member, IEEE,* Yangyang Zhang, and Chan-Byoung Chae, *Fellow, IEEE*

***Abstract*—Multiple access can be realized by utilizing the spatial moments of deep fades, using fluid antennas. The interference immunity for fluid antenna multiple access (FAMA), nevertheless, comes with the requirement of a large number of ports at each user. To alleviate this, we study the synergy between opportunistic scheduling and FAMA. A large pool of users permits selection of favourable users for FAMA and decreases the outage probability at each selected user. Our objective is to characterize the benefits of opportunistic scheduling in FAMA. In particular, we derive the multiplexing gain of the opportunistic FAMA network in closed form and upper bound the required number of users in the pool to achieve a given multiplexing gain. Also, we find a lower bound on the required outage probability at each user for achieving a given network multiplexing gain, from which the advantage of opportunistic scheduling is illustrated. In addition, we investigate the rate of increase of the multiplexing gain with respect to the number of users in the pool, and derive a tight approximation to the multiplexing gain, expressed in closed form. As a key result of our analysis, we obtain an operating condition on the product of the number of users in the pool and the number of ports at each fluid antenna that ensures a high multiplexing gain. Numerical results demonstrate clear benefits of opportunistic scheduling in FAMA networks, and corroborate our analytical results.**

***Index Terms*—Fluid antenna systems, Multiple Access, Multiplexing gain, Opportunistic scheduling, Spatial multiplexing.**

I. Introduction

A. Context

With SEVERAL generational changes, mobile communications has evolved into multi-functional communications over air that can combine with new features such as wireless power transfer [1], physical-layer security [2], mobile edge computing [3] and more. The past years have also seen overwhelming interest in applying machine learning methods in wireless communication systems, e.g., [4]–[7]. Despite the changes in emphasis on the applications, the push for greater spectral and energy efficiency has never changed.

The IMT-2020 Standard was motivated to meet the demands in three use cases with eight capabilities. One of the use cases is massive machine type communication (mMTC) which, for 5G, should provide connection density of 10^6 devices per km^2 [8]. Planning ahead of time, the ITU-R Working Party 5D has already begun to develop a new draft Recommendation "IMT Vision for 2030 and beyond". Though there has not been any consensus of what 6G will be, researchers around the world have speculated on the key performance indicators (KPIs) of 6G [9], [10]. To enable massive connectivity, multiple access technologies that allow an enormous number of users to share the same radio resource unit are of utmost importance.

Multiuser multiple-input multiple-output (MIMO), with its latest form as massive MIMO in 5G, has been a key enabling multiple access technology [11], [12]. By exploiting the channel state information (CSI) at the base station (BS), MIMO is able to differentiate and distribute the multiuser signals to the user equipments (UEs) in the downlink without interference. Nevertheless, the degree of freedom (DoF) is determined by the number of antennas at the BS, which is set by the standard and cannot be upgraded easily, not to mention the complexity and overhead associated with the CSI acquisition process and beamforming optimization. Another prevalent multiple access technology is non-orthogonal multiple access (NOMA) which promotes to overlap users even more beyond the capability of MIMO but requires successive interference cancellation (SIC) to be employed at the UEs [13], [14]. While NOMA is being portrayed as a massive connectivity technology, ironically, the majority of research is limited to only two-user cases.

Recently, it is proposed that spatial moments of deep fades can be exploited to eliminate interference and enable multiple access by a position-adjustable *fluid antenna* at a UE [15]. The idea is that signals intended for different UEs transmitted by distributed BS antennas undergo independent fading in space and hence, a UE equipped with high-resolution fluid antenna can access the deep fades suffered by its interference signals in space for multiple access without precoding nor SIC. Fluid antenna offers the possibility of massive connectivity with UE-led simple signal processing. Presumably, the network capacity can be increased if the resolution of fluid antenna at the UE side improves with time. It was reported that many users could be accommodated on the same time-frequency channel if the fluid antenna adapts its position on a symbol-by-symbol basis, an approach referred to as fast fluid antenna multiple access (f-FAMA) [16], [17] whereas supporting a few users on the same channel was still possible even if the fluid antenna only switched its position once in a coherence period, referred to as slow fluid antenna multiple access (s-FAMA) [18]–[20].

Fluid antennas can be implemented using liquid-based radiating structures [21], [22] or reconfigurable RF pixels [23]–[25]. Recent studies have seen many liquid-based reconfigurable antennas being designed, e.g., [26]–[30]. Latest devel-

The work of K. Wong and K. Tong is supported by the Engineering and Physical Sciences Research Council (EPSRC) under grants EP/T015985/1 and EP/W026813/1. For the purpose of open access, the authors will apply a Creative Commons Attribution (CC BY) licence to any Author Accepted Manuscript version arising.

The work of C. B. Chae is partly supported by the IITP grant funded by the Korean government (MSIT) (No. 2021-0-02208, No. 2021-0-00486).

The work of Y. Chen is supported by the National Natural Science Foundation of China under Grant 61901055.

K. K. Wong and K. F. Tong are with the Department of Electronic and Electrical Engineering, University College London, London WC1E 7JE, UK.

Y. Chen is with the School of Information and Communication Engineering (SICE), Beijing University of Posts and Telecommunications, China.

Y. Zhang is with Kuang-Chi Science Limited, Hong Kong SAR, China.

K. K. Wong and C. B. Chae are with School of Integrated Technology, Yonsei University, Seoul, Korea.

Corresponding author: Kai-Kit Wong.

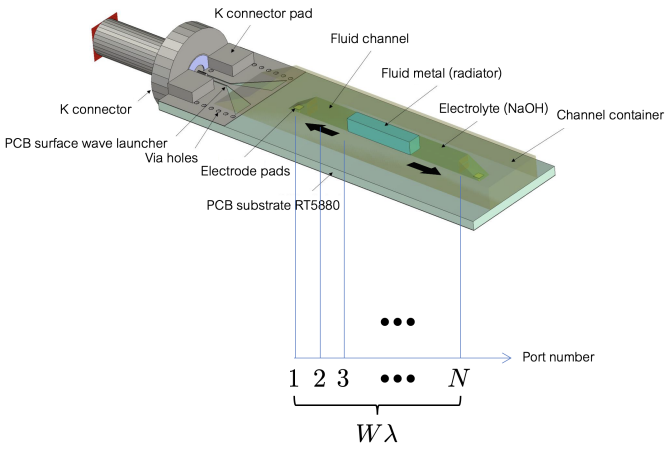

Fig. 1. The surface-wave based fluid antenna in [32].

opments also see surface wave communications being applied to increase the possible number of ports, i.e., resolution, of a fluid antenna [31], [32]. Most recently, [33] even discusses the prospect of having a fluid antenna array at mobile devices.

On the theoretical front, various performance metrics of a single-user fluid antenna system have been studied for different fading channels in [34]–[37]. Channel estimation in multiuser fluid antenna systems has also recently been tackled in [38]. Additionally, recently, movable antenna systems, a subbranch of fluid antenna systems, were also introduced for the single-input single-output (SISO) [39] and MIMO scenarios [40]. On the other hand, deep learning based algorithms have also been proposed to perform port selection efficiently for single-user fluid antenna systems [41] and s-FAMA systems [19]. In [20], it was even proposed to adopt extra-large MIMO to artificially create more fading for s-FAMA in millimeter-wave channels where there was line-of-sight and multipath was few.

Despite the strong multiple access capability, fluid antenna multiple access (FAMA) does require a large number of ports[1] to achieve the needed interference immunity. This appears to be a major limitation of FAMA since it would be practically very challenging to fit hundreds or even thousands of ports in the tiny space of a UE although the implementation challenge may be alleviated by distributing the ports over a 2D surface and/or utilizing the design in [31], [32]. It thus motivates us to investigate approaches that can make FAMA work when the number of ports, N, is not so large (say < 100). In particular, this paper combines FAMA and opportunistic scheduling.

Opportunistic scheduling is a powerful technique that takes advantage of multiuser diversity in deciding which users to be served at any given time [42]. Opportunism can even be utilized to match random beamforming to users if the pool of users is large enough [43]. Based on this principle, there is an obvious and simple synergy between opportunistic scheduling and FAMA. Presumably, FAMA can provide the protection to interference at the UEs while opportunistic scheduling plays a major role in selecting those UEs who can benefit most from the channels, thereby relaxing the required number of ports of the fluid antenna at each UE for multiple access.

[1]A 'port' refers to a fixated position to which the fluid radiating element can be switched. The number of ports dictates the resolution of a fluid antenna. Fig. 1 shows the surface-wave based fluid antenna in [32] with N ports.

B. Objectives

In this paper, we consider the opportunistic FAMA network where U best users are selected out of a pool of $M(\geq U)$ users based on their signal-to-interference ratios (SIRs) for FAMA. Our main objective is to quantify the benefits of opportunistic scheduling in FAMA by studying the multiplexing gain of the network, m. Lower bounds of the multiplexing gain will be obtained to gain insight on how the multiplexing gain scales with M and how M eases the requirement of the number of ports, N, for the fluid antenna at each UE for suppressing the interference to obtain a given performance. We will consider both f-FAMA [16] and s-FAMA [18] in the analysis.

C. Contributions and Summary of Results

Our contributions include a number of analytical results for the performance of the opportunistic FAMA network. We use order statistics to obtain the average network outage rate and thus the multiplexing gain when the outage probability of the fluid antenna, p, is given. Considering the case when Mp and $M(1-p)$ are reasonably large, Gaussian distribution is used to approximate the expression of the multiplexing gain, from which we investigate the impact of various system parameters such as the number of users in the pool, M, the number of selected users, U, the number of ports at each fluid antenna, N, and the size of the fluid antenna, $W\lambda$ where W denotes the normalized length and λ is the wavelength.

Before proceeding, we here provide an overall view of the material covered in this paper and highlight our key findings for the opportunistic FAMA systems.

- First, the average outage rate of the opportunistic FAMA network can be expressed as

$$C = \sum_{u=M-U+1}^{M} I_{1-p}(M-u+1,u)\log_2(1+\gamma),$$

in which $I_x(a,b)$ denotes the regularized incomplete beta function, and γ denotes the SIR threshold. Furthermore, the multiplexing gain can be found as

$$m = \sum_{u=M-U+1}^{M} I_{1-p}(M-u+1,u),$$

which, for large M, can be approximated by

$$m \approx \sum_{u=M-U+1}^{M} \left[1 - \frac{1}{2}\mathrm{erfc}\left(\frac{u-1-Mp}{\sqrt{2Mp(1-p)}}\right)\right],$$

where $\mathrm{erfc}(\cdot)$ is the complementary error function.
- For $0.0786U < m < 0.9214U$, it can be shown that the required outage probability achieved by the fluid antenna at each UE is lower bounded by

$$p \geq 1 - \frac{1}{M}\left(U + \alpha\sqrt{2U}\right),$$

where $\alpha \triangleq \text{erfc}^{-1}\left(2\left(1-\frac{m}{U}\right)\right)$ specifies the requirement of the multiplexing gain of the network.[2] Clearly, M has the role of reducing the burden of the fluid antenna when attempting to meet a given multiplexing gain, m.

- For f-FAMA with opportunistic scheduling, the number of ports at each UE's fluid antenna to meet a prescribed multiplexing gain is upper bounded by

$$N \leq \frac{1}{M}\left\lceil \frac{(U-1)\gamma}{1-\mu^2} \right\rceil (U+\alpha\sqrt{2U}),$$

where μ is the correlation parameter which depends on the size W of the fluid antenna. For the s-FAMA case, the result becomes

$$N \leq \frac{1}{M}\left(\frac{\gamma}{1-\mu^2}\right)^{U-1}(U+\alpha\sqrt{2U}).$$

For both FAMA scenarios, the results illustrate that the number of ports, N, is reduced by a factor of M.

- The rate of increase of the multiplexing gain, m, with respect to (w.r.t.) M can be derived as

$$\frac{\partial m}{\partial M} = \frac{1}{2\sqrt{2\pi}} \sum_{u=1}^{U} \frac{(1-p)M+u}{\sqrt{p(1-p)}} \left(\frac{e^{-\frac{[(1-p)M-u]^2}{2Mp(1-p)}}}{M^{\frac{3}{2}}} \right).$$

For very large M, it can further be shown that

$$\frac{\partial m}{\partial M} \propto \frac{e^{-\frac{[(1-p)M-U]^2}{2Mp(1-p)}}}{\sqrt{M}}.$$

- A rule of thumb for operating the opportunistic FAMA network efficiently is that the product of the number of UEs in the pool M and the number of ports at each UE's fluid antenna, N, should satisfy

$$MN > \begin{cases} \dfrac{U(U-1)\gamma}{1-\mu^2} & \text{if } f\text{-FAMA}, \\ U\left(\dfrac{\gamma}{1-\mu^2}\right)^{U-1} & \text{if } s\text{-FAMA}. \end{cases}$$

- Finally, the multiplexing gain can be accurately approximated as

$$m \approx \begin{cases} \min\left\{U, \dfrac{MN\left(1-\mu^2\right)}{(U-1)\gamma}\right\} & \text{if } f\text{-FAMA}, \\ \min\left\{U, MN\left(\dfrac{1-\mu^2}{\gamma}\right)^{U-1}\right\} & \text{if } s\text{-FAMA}. \end{cases}$$

D. Organization

The rest of the paper is organized as follows. In Section II, we introduce the model of the opportunistic FAMA network in the downlink and lay down our assumptions. Our main results will be presented in Section III while Section IV discusses the parameter selection. Section V then provides the numerical results that illustrate the benefits of the opportunistic FAMA networks. Finally, we conclude this paper in Section VI.

[2]Note that α does not have a convenient physical meaning but is defined mainly to simplify the expressions. With the range of the multiplexing gain $0.0786U < m < 0.9214U$ that α is defined, we have $-1 < \alpha < 1$.

II. Network Model

A. FAMA

We consider a downlink system where a multi-antenna BS is transmitting messages to U UEs on the same time-frequency resource unit. Each BS antenna is devoted to transmitting one UE's signal and the BS employs standard, fixed antennas. By contrast, each UE is equipped with a fluid antenna with a linear structure of length $W\lambda$ where λ denotes the wavelength. The fluid antenna has N ports (see an example in Fig. 1), to which the fluid radiating element can be switched, making it possible to receive the signal at N different, but close locations. The ports are distributed evenly over the space. For UE u, the received signal at the k-th port of fluid antenna is given by

$$r_k^{(u)} = s_u g_k^{(u,u)} + \underbrace{\sum_{\substack{\tilde{u}=1 \\ \tilde{u}\neq u}}^{U} s_{\tilde{u}} g_k^{(\tilde{u},u)} + \eta_k^{(u)}}_{\tilde{g}_k^{(u)}}, \tag{1}$$

in which s_u represents the transmitted symbol for user u with $\mathrm{E}[|s_u|^2] = \sigma_s^2$, $\eta_k^{(u)}$ is the zero-mean complex additive white Gaussian noise (AWGN) at the k-th port with $\mathrm{E}[|\eta_k^{(u)}|^2] = \sigma_\eta^2$, $g_k^{(\tilde{u},u)}$ is the fading channel from the BS antenna dedicated for transmitting UE $\tilde{u}$'s signal to the k-th port of UE u, and $\tilde{g}_k^{(u)}$ denotes the overall sum-interference plus noise signal at a symbol instant. Here, the time index is omitted for conciseness.

The amplitude of the channel, $|g_k^{(\tilde{u},u)}|$, is assumed Rayleigh distributed, with the probability density function (pdf)

$$p_{\left|g_k^{(\tilde{u},u)}\right|}(r) = re^{-\frac{r^2}{\sigma^2}}, \text{ for } r \geq 0 \text{ with } \mathrm{E}[|g_k^{(\tilde{u},u)}|^2] = 2. \tag{2}$$

The average received signal-to-noise ratio (SNR) at each port is given by $\Gamma = \frac{2\sigma_s^2}{\sigma_\eta^2}$. As the ports can be arbitrarily close to each other, the channels $\{g_k^{(\tilde{u},u)}\}_{\forall k}$ are correlated. To account for the channel correlation, we parameterize $g_k^{(\tilde{u},u)}$, through a single correlation parameter μ, as [44]

$$g_k^{(\tilde{u},u)} = \left(\sqrt{1-\mu^2}x_k^{(\tilde{u},u)} + \mu x_0^{(\tilde{u},u)}\right) + j\left(\sqrt{1-\mu^2}y_k^{(\tilde{u},u)} + \mu y_0^{(\tilde{u},u)}\right), \quad k = 1,2,\ldots,N, \tag{3}$$

where $x_0^{(\tilde{u},u)}, \ldots, x_N^{(\tilde{u},u)}, y_0^{(\tilde{u},u)}, \ldots, y_N^{(\tilde{u},u)}$ are all independent Gaussian random variables with zero mean and variance of 1. Using this model, the correlation among the ports is realized through the common random variables $x_0^{(\tilde{u},u)}$ and $y_0^{(\tilde{u},u)}$. The parameter μ serves to control the amount of spatial correlation between any two ports of the fluid antenna. Specifically, with a linear structure of $W\lambda$, μ can be chosen such that

$$\mu = \sqrt{2}\sqrt{{}_1F_2\left(\frac{1}{2}; 1, \frac{3}{2}; -\pi^2W^2\right) - \frac{J_1(2\pi W)}{2\pi W}}, \tag{4}$$

where ${}_aF_b(\cdot;\cdot;\cdot)$ denotes the generalized hypergeometric function and $J_1(\cdot)$ is the first-order Bessel function of the first kind.

Setting μ using (4) achieves the same mean correlation coefficient for an N-port linear structure of length $W\lambda$ [44, Theorem 1]. According to [44, Theorem 2], μ can be approximated as

$$\mu \approx \begin{cases} 1 - \dfrac{\pi^2 W^2}{12}, & \text{for } W \leq 0.6, \\ \dfrac{1}{\sqrt{\pi W}}, & \text{for } W \geq 1. \end{cases} \tag{5}$$

Since the performance of the network will be interference-limited, we can drop the noise in our analysis. To benefit from the fluid antenna, UE u can select the best port for maximizing the SIR for communications. For f-FAMA, it is proposed to track the sum-interference null on a symbol-by-symbol basis so that the selection can be done by [16], [17]

$$k_u^{f\text{-FAMA}} = \arg \max_{k \in \{1,\ldots,N\}} \frac{\left|g_k^{(u,u)}\right|^2}{\left|\tilde{g}_k^{(u)}\right|^2}. \tag{6}$$

By contrast, s-FAMA only updates the ports of the users if the fading channels change. In this case, it chooses [18]

$$k_u^{s\text{-FAMA}} = \arg \max_{k \in \{1,\ldots,N\}} \frac{\left|g_k^{(u,u)}\right|^2}{\sum_{\substack{\tilde{u}=1 \\ \tilde{u}\neq u}}^{U} \left|g_k^{(\tilde{u},u)}\right|^2}. \tag{7}$$

The various challenges of performing (6) and (7) and how they may be addressed have been discussed in [15].

An important performance metric for the FAMA network is the outage probability of the resulting SIR of the selected port for a typical user. In our model, the UEs are independent and identically distributed (i.i.d.) and hence have the average outage probability, p, which specifies the interference immunity of a typical UE. By definition, we have

$$p = \mathrm{E}_u \left[\mathrm{Prob}\left(\mathrm{SIR}_u = \max_{k \in \{1,\ldots,N\}} \mathrm{SIR}_{u,k} < \gamma \right) \right], \tag{8}$$

in which γ denotes the SIR threshold and $\mathrm{SIR}_{u,k}$ denotes the SIR at the k-th port of UE u. As such, SIR_u represents the resulting SIR at the best port at UE u.[3] The outage probability expressions for the f-FAMA and s-FAMA cases can be found as (9) [44, (17)] and (10) [18, (21)], respectively, where $I_k(\cdot)$ is the modified Bessel function of the first kind, $Q_m(\cdot,\cdot)$ is the generalized Marcum-Q function, $(a)_j$ is the Pochhammer symbol, and $\Gamma(n) = (n-1)!$ is the gamma function.

For the typical case $W > 1$, the outage probability expressions can be simplified using first-order approximations, [45, Theorem 1] and [18, Theorem 3] so that

$$p \approx \begin{cases} \left[1 - \dfrac{N\left(1-\mu^2\right)}{(U-1)\gamma}\right]^+ & \text{if } f\text{-FAMA}, \\ \left[1 - N\left(\dfrac{1-\mu^2}{\gamma}\right)^{U-1}\right]^+ & \text{if } s\text{-FAMA}, \end{cases} \tag{11}$$

where $[a]^+ = \max(0, a)$ and $\mu^2 \approx \frac{1}{\pi W}$ can be used.

[3]While SIR indeed means the signal to interference ratio averaged over data in s-FAMA, for the case of f-FAMA, we have abused the notation 'SIR' to include the meaning of the ratio of the instantaneous energy of the desired signal to that of the sum-interference plus noise signal.

B. Opportunistic Scheduling

We consider that the U users selected for communications on the same time-frequency resource unit are based on their SIRs, see Fig. 2. In particular, it is assumed that there are $M(>U)$ UEs in the pool and their SIRs are ranked, i.e.,

$$\mathrm{SIR}^{(1)} \leq \mathrm{SIR}^{(2)} \leq \cdots \leq \mathrm{SIR}^{(M)}, \tag{12}$$

in which $\mathrm{SIR}^{(u)}$ represents the SIR of the best port of the u-th weakest UE (or the $(M-u+1)$-th strongest UE) in the pool. In particular, the strongest $U(<M)$ UEs are selected to communicate at any given time. Therefore, we have

$$\mathrm{SIR}^{(M-U+1)} \leq \mathrm{SIR}^{(M-U+2)} \leq \cdots \leq \mathrm{SIR}^{(M)}. \tag{13}$$

As in previous work [16], [18], [44], [45], the UEs' messages are transmitted with a common fixed coding rate specified by the SIR target γ, i.e., $R = \log_2(1+\gamma)$. As a consequence, we define a UE's 'capacity' as the average outage rate as follows.

Definition 1: The capacity for UE u is defined as

$$C_u = \left[1 - \mathrm{Prob}(\mathrm{SIR}_u < \gamma)\right] \log_2(1+\gamma). \tag{14}$$

Opportunistic scheduling for selecting the best U users from a pool of M users is well motivated to

$$\max_{j(\cdot)} \sum_{u=1}^{U} C_{j(u)}, \tag{15}$$

by finding the function $j(\cdot)$ that selects the best users, where $C_{j(u)}$ represents the average outage rate for the u-th strongest user. Note that we have $\mathrm{SIR}^{(M-u+1)} = \mathrm{SIR}_{j(u)}$.

In general, the SIR of a UE depends on other selected users which means that in theory, all $\binom{M}{U}$ combinations will need to be checked in order to truly find the U strongest UEs. This nonetheless would be practically impossible to do. Fortunately, in FAMA, no BS preprocessing specific to the selected users is needed, meaning that the outage probability performance of any selected UE does not depend on any other selected UEs. As a result, a UE can establish the confidence level on whether it is ranked in the top U in the pool given the UE's SIR. Thus, it is possible for the BS to sequentially turn on and off UEs until the top UEs are identified. While such selection method is possible and deserves further investigation, in this paper, we will always assume that the strongest U UEs are selected.

It is worth pointing out that FAMA does expect each UE's channel envelope not to change too fast to work. Each UE will need to find and switch to the best port for communications. If the CSI changes too quickly due to high mobility, then it would be difficult for a UE to figure out the best port in time to avoid interference although recent studies have led to efficient port selection algorithms for f-FAMA [17] and s-FAMA systems [19]. If opportunistic scheduling is to be used with FAMA, then it is even more reasonable to consider low-mobility UEs because the U best UEs might change over time. That said, since we target massive connectivity scenarios, it makes sense to consider primarily low-mobility UEs as traditionally about $70-80\%$ of mobile data traffic is generated indoors (including traffic served by in-building systems). In addition, for high-mobility UEs, multiple access techniques such as interleave division multiple access (IDMA) [46] or code division multiple

$$p=\int_0^\infty e^{-z}\int_0^\infty e^{-t}\left[1+\left(\frac{(U-1)\gamma}{(U-1)\gamma+1}\right)e^{-\left(\frac{1}{(U-1)\gamma+1}\right)\frac{\mu^2}{1-\mu^2}((U-1)\gamma z+t)}I_0\left(\frac{\sqrt{(U-1)\gamma}}{(U-1)\gamma+1}\left(\frac{2\mu^2}{1-\mu^2}\right)\sqrt{zt}\right)\right.$$
$$\left.-Q_1\left(\frac{1}{\sqrt{(U-1)\gamma+1}}\sqrt{\frac{2\mu^2}{1-\mu^2}}\sqrt{t},\frac{\sqrt{(U-1)\gamma}}{\sqrt{(U-1)\gamma+1}}\sqrt{\frac{2\mu^2}{1-\mu^2}}\sqrt{z}\right)\right]^N dtdz \quad (9)$$

$$p=\int_0^\infty\int_0^\infty\frac{\tilde{r}^{U-2}}{2^U\Gamma(U-1)}e^{-\frac{r+\tilde{r}}{2}}\left\{Q_{U-1}\left(\frac{\mu}{\sqrt{1-\mu^2}}\sqrt{\frac{\gamma\tilde{r}}{\gamma+1}},\frac{\mu}{\sqrt{1-\mu^2}}\sqrt{\frac{r}{\gamma+1}}\right)\right.$$
$$-\left(\frac{1}{\gamma+1}\right)^{U-1}e^{-\frac{\mu^2}{2(1-\mu^2)}\left(\frac{\gamma\tilde{r}+r}{\gamma+1}\right)}\times$$
$$\left.\sum_{k=0}^{U-2}\sum_{j=0}^{U-k-2}\frac{(U-(j+k)-1)_j}{j!}\left(\frac{r}{\tilde{r}}\right)^{\frac{j+k}{2}}(\gamma+1)^k\gamma^{\frac{j-k}{2}}I_{j+k}\left(\frac{\mu^2}{1-\mu^2}\frac{\sqrt{\gamma r\tilde{r}}}{(\gamma+1)}\right)\right\}^N drd\tilde{r} \quad (10)$$

access (CDMA) [47] are well known to work well. In fact, the low-mobility case which suffers from slow channel fading has long been regarded as the more challenging case to tackle.

III. Multiplexing Gain Analysis

In this section, we present our main results that characterizes the performance of opportunistic FAMA networks. We mainly focus upon the multiplexing gain analysis because it uncovers the capacity scaling achievable from integrating opportunistic scheduling and FAMA. Following the UE's capacity definition, we define the network capacity below.

Definition 2: The network capacity is defined as

$$C=\sum_{u=M-U+1}^{M}(1-q_u)\log_2(1+\gamma), \quad (16)$$

where

$$q_u=\text{Prob}(\text{SIR}^{(u)}<\gamma) \quad (17)$$

denotes the outage probability of the u-th weakest UE.

Note that C in (16) uses the fact that the U strongest UEs are selected for FAMA communications.

The following theorem presents the expression for q_u.

Theorem 1: The SIR outage probability with an SIR threshold, γ, for the u-th weakest FAMA user is given by

$$q_u=\sum_{k=u}^{M}\binom{M}{k}p^k(1-p)^{M-k}, \quad (18)$$

where p is given by (9) for f-FAMA and (10) for s-FAMA. Furthermore, q_u can be rewritten as

$$q_u\overset{(a)}{=}I_p(u,M-u+1)\overset{(b)}{=}1-I_{1-p}(M-u+1,u), \quad (19)$$

where $I_x(a,b)$ is the regularized incomplete beta function.

Proof: Given the SIR outage probability for a typical UE and using order statistics [48] get the result (18). Then (a) and (b) in (19) come directly from the properties of the probability of a binomial random variable. ■

Corollary 1: The network outage rate of the opportunistic FAMA network is given by

$$C=\sum_{u=M-U+1}^{M}I_{1-p}(M-u+1,u)\log_2(1+\gamma). \quad (20)$$

Proof: Combining (16) and (19) gets the result. ■

Theorem 2: The multiplexing gain, m, of the opportunistic FAMA network is given by

$$m\overset{(a)}{=}\sum_{u=M-U+1}^{M}I_{1-p}(M-u+1,u) \quad (21a)$$
$$\overset{(b)}{\approx}\sum_{u=M-U+1}^{M}\left[1-\frac{1}{2}\text{erfc}\left(\frac{u-1-Mp}{\sqrt{2Mp(1-p)}}\right)\right] \quad (21b)$$
$$\overset{(c)}{>}UI_{1-p}(U,M-U+1) \quad (21c)$$
$$\overset{(d)}{\approx}U\left[1-\frac{1}{2}\text{erfc}\left(\frac{(1-p)M-U}{\sqrt{2Mp(1-p)}}\right)\right], \quad (21d)$$

where $\text{erfc}(\cdot)$ is the complementary error function.

Proof: As the multiplexing gain measures the capacity scaling of the network, m is obtained by dividing C in (20) by the coding rate of a single user with zero outage probability because of the absence of interference, which gives (21a). The result (21b) is derived by approximating the binomial random variable using a Gaussian random variable if M is large such that $Mp>5$ and $M(1-p)>5$. The lower bound (21c) is obtained by replacing all the terms in (21b) by the probability of the weakest UE out of U strongest UEs. Finally, (21d) is due to Gaussian approximation, which completes the proof. ■

The next theorem provides a conservative estimate on the required number of UEs in the selection pool, M for achieving particular regions of the multiplexing gain, m.

Theorem 3: To achieve a given multiplexing gain, m, which is specified by the parameter

$$\alpha\triangleq\text{erfc}^{-1}\left[2\left(1-\frac{m}{U}\right)\right], \quad (22)$$

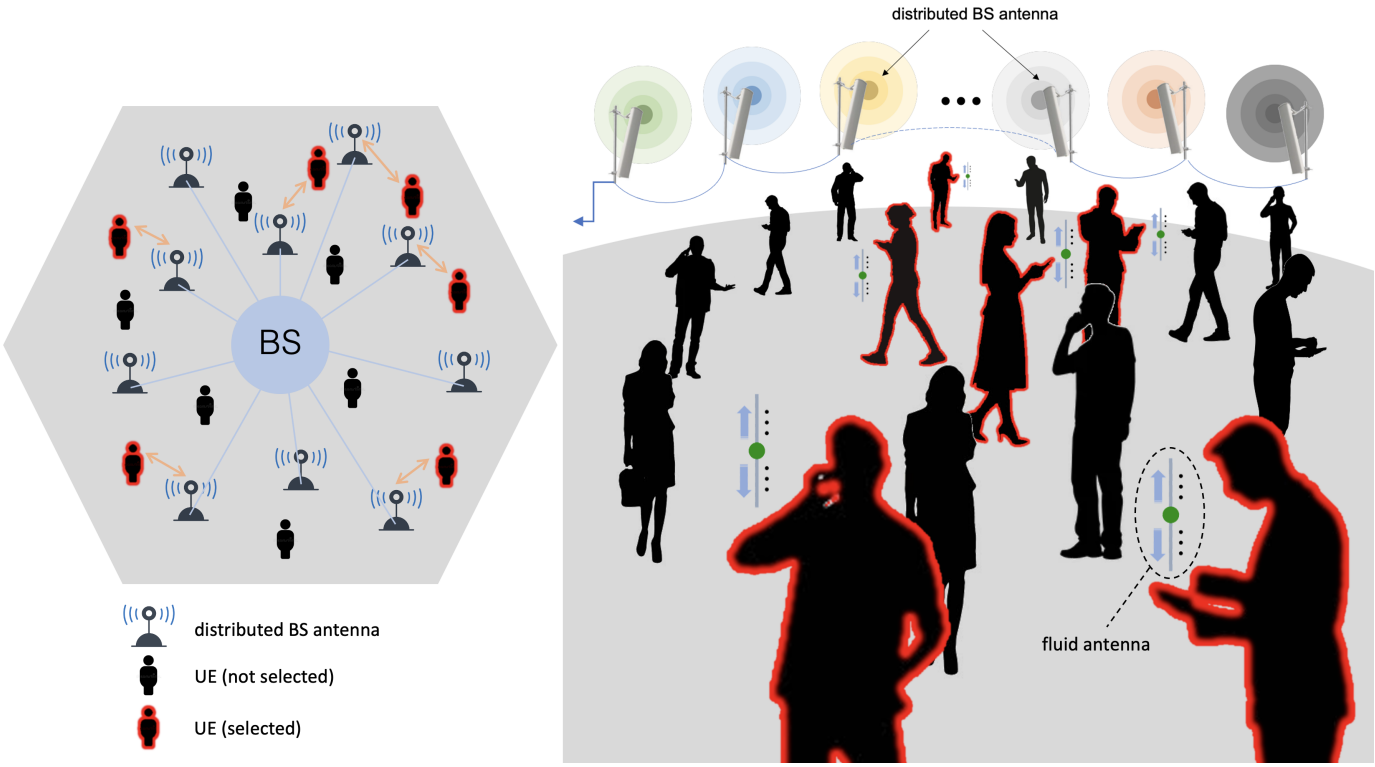

Fig. 2. Illustration of an opportunisic FAMA system in the downlink where a subset of UEs are highlighted and selected for communications on the same time-frequency channel using their fluid antennas. The BS uses distributed antennas, each of which is dedicated to transmit information to one designated UE. Left: The schematic of the opportunistic FAMA network with distributed BS antennas; Right: A high-level abstract illustration.

the required number of users in the pool, M, is bounded by

$$M \leq \frac{U + \alpha^2 p - \sqrt{(\alpha^2 p)(\alpha^2 p + 2U)}}{1-p} \text{ for } 0 \leq m \leq \frac{U}{2}, \tag{23}$$

and for $\frac{U}{2} \leq m \leq U$, we have

$$\frac{U}{1-p} \leq M \leq \frac{U + \alpha^2 p + \sqrt{(\alpha^2 p)(\alpha^2 p + 2U)}}{1-p}. \tag{24}$$

Proof: See Appendix A. ■

Theorem 3 gives a conservative estimate on upper bounding M for achieving a given multiplexing gain m. An observation of the results reveals that a smaller p will have a smaller upper bound on M as expected. The following theorem attempts to understand the requirement on the interference immunity of the fluid antenna at a typical UE. In so doing, we illustrate the benefits of M in the opportunistic FAMA network.

Theorem 4: To achieve a given multiplexing gain such that

$$0.0786U \approx \left[1 - \frac{\text{erfc}(-1)}{2}\right] U < m < \left[1 - \frac{\text{erfc}(1)}{2}\right] U \approx 0.9214U, \tag{25}$$

the outage probability, p, of each of the UEs in the opportunistic FAMA network can be lower bounded by

$$p \geq 1 - \frac{1}{M}(U + \alpha\sqrt{2U}). \tag{26}$$

Proof: See Appendix B. ■

Notice that the above theorem is based on the lower bound (21d), meaning that (26) cannot be very accurate and should somewhat be conservative. Thus, the importance of Therorem 4 lies in that it illustrates the impact of M on the requirement of the interference immunity at the fluid antenna of each user. In particular, we see that as M increases, the right hand side of (26) approaches one, which indicates that each UE is left with not much to do in eliminating the multiuser interference and the capacity scaling will be very good. On the other hand, it is true that Therorem 4 does not cover the full range of m in the analysis. Nonetheless, when $m < 0.0786U$, the network would not be functioning properly at all and this case will not be useful. On the other hand, since the result in Therorem 4 is derived from (21d), the actual achievable multiplexing gain, m, will exceed the range beyond $m > 0.9214U$.

Theorem 5: For f-FAMA, the required number of ports, N, at the fluid antenna at each UE is upper bounded by

$$N \leq \frac{1}{M}\left[\frac{(U-1)\gamma}{1-\mu^2}\right](U + \alpha\sqrt{2U}), \tag{27}$$

in order to meet a given multiplexing gain requirement specified by α. For $W \geq 1$, the result can be expressed as

$$N \leq \frac{1}{M}\left[\frac{(U-1)\gamma}{1-\frac{1}{\pi W}}\right]\left(U + \text{erfc}^{-1}\left[2\left(1-\frac{m}{U}\right)\right]\sqrt{2U}\right). \tag{28}$$

Proof: Using (11) and applying Therorem 4, we have

$$1 - \frac{N(1-\mu^2)}{(U-1)\gamma} \geq 1 - \frac{1}{M}(U + \alpha\sqrt{2U}), \tag{29}$$

which after some rearrangement, then gives (27). Note that the operation $[\cdot]^+$ in (11) is omitted as we assume the scenario $N < \frac{(U-1)\gamma}{1-\mu^2}$. Finally, (28) is obtained after we have employed the definition of α and used the approximation (5). ∎

Theorem 6: For s-FAMA, the required number of ports, N, at the fluid antenna at each UE is upper bounded by

$$N \leq \frac{1}{M}\left(\frac{\gamma}{1-\mu^2}\right)^{U-1}(U+\alpha\sqrt{2U}), \tag{30}$$

in order to meet a given multiplexing gain requirement specified by α. For $W \geq 1$, the result can be expressed as

$$N \leq \frac{1}{M}\left(\frac{\gamma}{1-\frac{1}{\pi W}}\right)^{U-1}\left(U+\text{erfc}^{-1}\left[2\left(1-\frac{m}{U}\right)\right]\sqrt{2U}\right). \tag{31}$$

Proof: The results can be proved similarly as before. ∎

Apparently, both Theorem 5 and Theorem 6 reveal that the upper bound on the required number of ports, N, is inversely proportional to M, meaning that M can help bring down the requirements of the fluid antenna at each UE. In the extreme case when $M \to \infty$, N can be made arbitrarily small.

While M clearly plays a major role in relieving the pressure of the fluid antenna at each UE, it is anticipated that increasing M increases the multiplexing gain of the opportunistic FAMA network when N is fixed. The following theorem characterizes the rate at which m is increased with M.

Theorem 7: The rate of change of the multiplexing gain w.r.t. the number of users in the pool is given by

$$\frac{\partial m}{\partial M} = \frac{1}{2\sqrt{2\pi}}\sum_{u=1}^{U}\left[\frac{(1-p)M+u}{\sqrt{p(1-p)}}\right]\frac{e^{-\frac{[(1-p)M-u]^2}{2Mp(1-p)}}}{M^{\frac{3}{2}}}. \tag{32}$$

Proof: We start by rewriting (21b) as

$$\begin{aligned} m &\approx \sum_{u=M-U+1}^{M}\left[1-\frac{1}{2}\text{erfc}\left(\frac{u-1-Mp}{\sqrt{2Mp(1-p)}}\right)\right] \\ &= U-\frac{1}{2}\sum_{u=1}^{U}\text{erfc}\left(\frac{(1-p)M-u}{\sqrt{2Mp(1-p)}}\right). \end{aligned} \tag{33}$$

Knowing that $\frac{\text{derfc}(x)}{dx} = -\frac{2e^{-x^2}}{\sqrt{\pi}}$, we can find that

$$\begin{aligned} &\frac{\partial}{\partial M}\left[\text{erfc}\left(\frac{(1-p)M-u}{\sqrt{2Mp(1-p)}}\right)\right] \\ &\qquad = -\frac{(1-p)M+u}{\sqrt{2\pi}\sqrt{p(1-p)}}\frac{e^{-\frac{[(1-p)M-u]^2}{2Mp(1-p)}}}{M^{\frac{3}{2}}}. \end{aligned} \tag{34}$$

Differentiating (33) w.r.t. M and using (34) get (32). ∎

Corollary 2: For very large M, it can be found that

$$\frac{\partial m}{\partial M} \approx \frac{1}{2\sqrt{2\pi}}\sqrt{\frac{1-p}{p}}\frac{e^{-\frac{[(1-p)M-U]^2}{2Mp(1-p)}}}{\sqrt{M}}. \tag{35}$$

Proof: The result can be obtained directly from (32) after considering M to be very large. ∎

Corollary 3: If

$$M > \frac{U}{1-p}, \tag{36}$$

then the increase in the multiplexing gain will plateau, and any further increase in M will have a diminishing return. Hence, (36) provides a useful condition to decide on the effective M for the best performance of the opportunistic FAMA network.

Proof: When (36) is held, it can be observed from (35) in Corollary 2 that $\frac{\partial m}{\partial M} \approx 0$ and therefore, M saturates. ∎

Corollary 4: For an effective operation of the opportunistic FAMA network, one should choose the parameters to satisfy

$$MN > \begin{cases} \dfrac{U(U-1)\gamma}{1-\mu^2} & \text{if } f\text{-FAMA}, \\ U\left(\dfrac{\gamma}{1-\mu^2}\right)^{U-1} & \text{if } s\text{-FAMA}. \end{cases} \tag{37}$$

For $W \geq 1$, we can further express the result in terms of the size of the fluid antenna, W, as

$$MN > \begin{cases} \dfrac{U(U-1)\gamma}{1-\frac{1}{\pi W}} & \text{if } f\text{-FAMA}, \\ U\left(\dfrac{\gamma}{1-\frac{1}{\pi W}}\right)^{U-1} & \text{if } s\text{-FAMA}. \end{cases} \tag{38}$$

Proof: The result (37) comes directly from the condition in Corollary 3 when the outage probability results in (11) are substituted. When $W \geq 1$, we use (5) to get (38). ∎

Corollary 4 provides a simple condition on the parameters of the opportunistic FAMA network that strikes a good balance between capacity performance and complexity. It inherently seeks to achieve the highest increase in capacity scaling as the number of users in the pool is increased.

Corollary 5: As $M \to \infty$,

$$m \to U. \tag{39}$$

Proof: For very large M, it can be seen that

$$\text{erfc}\left(\frac{(1-p)M-u}{\sqrt{2Mp(1-p)}}\right) \approx \text{erfc}\left(\sqrt{\frac{1-p}{2p}}\sqrt{M}\right), \tag{40}$$

which goes to 0 if $M \to \infty$. Then taking the limit $M \to \infty$ and using the above result in (33) obtains (39). ∎

Theorem 8: For large M, the multiplexing gain, m, of the opportunistic FAMA network can be approximated by

$$m \approx U\left[1-\frac{1}{\sqrt{2\pi}}\sqrt{\frac{p}{1-p}}\frac{e^{-\left(\frac{1-p}{2p}\right)M}}{\sqrt{M}}\right]. \tag{41}$$

Proof: For large x, we have the Taylor series

$$\begin{aligned} \text{erfc}(a\sqrt{x}) &= \frac{e^{-a^2x}}{a}\times \\ &\left(\frac{x^{-0.5}}{\sqrt{\pi}}-\frac{x^{-1.5}}{2a^2\sqrt{\pi}}+\frac{3x^{-2.5}}{4a^4\sqrt{\pi}}-\frac{15x^{-3.5}}{8a^6\sqrt{\pi}}+\cdots\right). \end{aligned} \tag{42}$$

Applying the above result while keeping only the term $x^{-0.5}$ (i.e., for large M), we can get

$$\text{erfc}\left(\sqrt{\frac{1-p}{2p}}\sqrt{M}\right) \approx \frac{1}{\sqrt{\pi}}\sqrt{\frac{2p}{1-p}}\frac{e^{-\left(\frac{1-p}{2p}\right)M}}{\sqrt{M}}. \tag{43}$$

Now, using this result in (33) obtains the desired result. ∎

Theorem 8 provides a succinct expression to illustrate how the multiplexing gain of the network grows with the number of

users in the pool when M is very large. Despite its simplicity, it may not be accurate when M is not much greater than U. Even if M is indeed much greater than U, then $m \approx U$, which makes the expression (41) quite unnecessary. For this reason, the following theorem is presented to provide an estimate on m for the case when M is not much greater than U.

Theorem 9: For $M \geq U$, the multiplexing gain, m, of the opportunistic FAMA network can be approximated by (44) (see top of next page) in which $U_0 = U$ if $M \geq \frac{U}{1-p}$ and if $M < \frac{U}{1-p}$, then U_0 is selected such that

$$U \geq U_0 + 1 > (1-p)M > U_0 \text{ or } U_0 = \lfloor (1-p)M \rfloor, \quad (45)$$

where $\lfloor z \rfloor$ returns the largest integer which is smaller than z.

Proof: See Appendix C. ∎

Theorem 10: The multiplexing gain, m, of the opportunistic FAMA network can be accurately approximated by

$$m \approx \min\left\{U, M(1-p)\right\}, \quad (46)$$

where $m \approx U$ if $p < 1 - \frac{U}{M}$ and $m \approx M(1-p)$ otherwise.

Proof: See Appendix D. ∎

Corollary 6: In the linear region, the multiplexing gain, m, of the opportunistic FAMA network can be written as

$$m = \begin{cases} \dfrac{MN\left(1-\mu^2\right)}{(U-1)\gamma} & \text{if } f\text{-FAMA}, \\ MN\left(\dfrac{1-\mu^2}{\gamma}\right)^{U-1} & \text{if } s\text{-FAMA}. \end{cases} \quad (47)$$

Proof: Using (46) and (11) yields the result. ∎

IV. System Parameter Selection

The analysis in the previous section helps understand how various system parameters contribute to the overall capacity performance of opportunistic FAMA networks. Here, we discuss how the parameters may be chosen, with the help of the analytical results. We go through the key parameters below.

- **The number of ports at the fluid antenna of each UE,** N—This represents the resolution the fluid antenna has to explore the fading channel in space. The larger the number of ports, the higher the precision and the better the interference rejection ability at each UE.
- **The normalized size of the fluid antenna,** W—This represents the spatial coverage the fluid antenna has to experience the different fading variations in space. The larger the size, the higher the diversity of the channel and the better the performance at each UE.
- **The SIR threshold,** γ—This specifies the quality-of-service (QoS) of the UE that is related to the particular type of communication, and is usually given.
- **The number of UEs in the selection pool for scheduling,** M—This dictates the amount of multiuser diversity we can obtain and represents the total number of users that the network can access the physical layer performance measures at any one time for scheduling. The larger the value of M, the better the performance.
- **The number of selected UEs,** U**, for communication at any given time**—This represents the number of users to be selected for sharing the same time-frequency resource unit at each schedule. The larger the value of U, the more the interference each selected UE suffers but potentially the higher the network capacity if the fluid antenna at each UE is powerful enough to handle the interference.

Note that N should be chosen as large as possible according to the hardware design and constraint while W is another hardware parameter that again should be as large as possible depending on the available space of the device. Additionally, γ is usually prescribed based on the required QoS of the UE. Furthermore, M should be chosen as large as practically possible for the best performance regardless of the network conditions. Lastly, U appears to be the trickiest parameter that should be optimized according to the interplay between the amount of interference suffered at each UE and the overall network capacity (or multiplexing gain).

The optimization of U can be performed with the help of Corollary 4 and Corollary 5. We use f-FAMA as an example to show how this is conducted. First, according to Corollary 5, the maximum limit of the multiplexing gain is U meaning that U should be maximized if possible for greater network capacity. However, according to Corollary 4, given M, N, γ and $W(\geq 1)$, U should satisfy

$$MN > \frac{U(U-1)\gamma}{1-\frac{1}{\pi W}} \Rightarrow U^2 - U - \frac{MN}{\gamma}\left(1 - \frac{1}{\pi W}\right) < 0. \quad (48)$$

As a result, U should be found by

$$\max U \text{ s.t. } U^2 - U - \frac{MN}{\gamma}\left(1 - \frac{1}{\pi W}\right) < 0. \quad (49)$$

It can be easily shown that

$$U_{\text{opt}} = \left\lfloor \frac{1 + \sqrt{\frac{4MN}{\gamma}\left(1 - \frac{1}{\pi W}\right) + 1}}{2} \right\rfloor. \quad (50)$$

The case for s-FAMA can be addressed similarly.

V. Numerical Results

Here, we provide the numerical results to evaluate the multiplexing gain performance of the opportunistic FAMA network and attempt to gain some useful insight on its operation. Note that the multiplexing gain, m, illustrates the capacity scaling of the network over a single-user system occupying the same bandwidth. This performance metric depends on three crucial parameters, U, M and p while p is a function of the parameters of the fluid antenna at each UE such as its size W, the SIR threshold γ and the number of ports N. Figs. 3 and 4 make observations on m against the system parameters U, M and p while Fig. 5 attempts to unpack the impact of the parameters of the fluid antenna for both f-FAMA and s-FAMA cases.

In Figs. 3 and 4, the exact results (21a) and the approximations (33) and (44) are provided. The results illustrate that the results for (33) and (44) coincide, which indicates that the approximation (44) to (33) is extremely accurate whereas the accuracy of the approximations to (21a) improves greatly as U increases. Even if U is not so large (e.g., $U = 5, 10$), the approximations can pick up the trend of m very well but they

$$m \approx U_0 - \frac{1}{B}\sqrt{\frac{Mp(1-p)}{2\pi}}\sum_{u=1}^{U}\frac{e^{-\frac{[(1-p)M-u]^2}{2Mp(1-p)}}}{(1-p)M-u} + \frac{1}{B}\sqrt{\frac{Mp(1-p)}{2\pi}}\left[\sum_{u=1}^{U_0}\frac{e^{-\frac{A[(1-p)M-u]}{\sqrt{2Mp(1-p)}}}e^{-\frac{[(1-p)M-u]^2}{2Mp(1-p)}}}{(1-p)M-u} + \sum_{u=U_0+1}^{U}\frac{e^{\frac{A[(1-p)M-u]}{\sqrt{2Mp(1-p)}}}e^{-\frac{[(1-p)M-u]^2}{2Mp(1-p)}}}{(1-p)M-u}\right] \quad (44)$$

tend to give a lower bound of the multiplexing gain. Also, we observe that as expected, the maximum multiplexing gain in all the cases is U. As M increases, m increases considerably demonstrating the effectiveness of opportunistic scheduling in FAMA. In a similar fashion, reducing p using more powerful fluid antennas increases m greatly. Thus the synergy between opportunistic scheduling and FAMA is significant. Moreover, a close observation of the results in Fig. 3 confirms that m exhibits a linear relationship with M and saturates sharply if $M > \frac{U}{1-p}$, as predicted in Corollary 3. For example, for the case $U = 100$, Corollary 3 predicts that $M > \frac{U}{1-p} = \frac{100}{1-0.5} = 200$ is the point at which m begins to plateau, which is exactly what is observed in the figure. In other words, the result of Theorem 10 (or the approximation (46)) is validated.

Results of Fig. 4 are plotted against the outage probability at each fluid antenna in the x-axis. In the figure, we also include vertical lines that specify $p = 1 - \frac{U}{M}$, the point at which $m \approx M$ occurs as predicted by Corollary 3. Apparently, a larger M can relax the requirement on p for approaching $m \approx U$. The results reveal some attractive operations of the opportunistic FAMA network. For example, if $U = 5$ and $M = 8$, we can achieve $m \approx 4.5$ at $p = 0.375$ (achievable by a fluid antenna with 1000 ports using s-FAMA [18, Fig. 2]). On the other hand, if $U = 100$ and $M = 150$, then we can obtain $m \approx 98$ at $p = 0.3333$ (achievable by a fluid antenna with 1120 ports using f-FAMA). Lastly, the results in this figure again confirm that the approximations we have derived are accurate.

We conclude this section by examining the results in Fig. 5 in which the network multiplexing gain is plotted against the parameters of the fluid antenna at each UE for both f-FAMA (Fig. 5(a)) and s-FAMA (Fig. 5(b)) cases. The f-FAMA case refers to the more advanced and complex setup of fluid antenna (hence able to accommodate a large number of UEs; $U = 50$) while the s-FAMA case is a more practical setup (supporting a less number of UEs at much lower complexity; $U = 4$). As can be observed, if $U = M$, i.e., no opportunistic scheduling is employed, then it will require an extraordinarily large number of ports, N, to approach $m \approx U$, see Fig. 5(a)(i) & (b)(i). The increase in the number of users in the selection pool, M, helps greatly reduce the requirement on N, which can bring the required N from thousands to hundreds. According to (38) in Corollary 4, $m \approx U$ if

$$N > \begin{cases} \dfrac{U(U-1)\gamma}{M\left(1-\frac{1}{\pi W}\right)} & \text{if } f\text{-FAMA}, \\ \dfrac{U}{M}\left(\dfrac{\gamma}{1-\frac{1}{\pi W}}\right)^{U-1} & \text{if } s\text{-FAMA}. \end{cases} \quad (51)$$

This predicts that for f-FAMA, if $U = 50$, $M = 110$, $\gamma = 10$dB and $W = 2$, then m will begin to plateau when $N > 265$, which agrees with the numerical results. We notice that the prediction for s-FAMA is less accurate in the numerical results and this is because the analysis leading to (38) is based on the assumption that γ is large and in the case of s-FAMA, we have chosen $\gamma = 5$dB and thus affected the accuracy.

Figs. 5(a)(ii) & (b)(ii) investigate how the multiplexing gain varies when the SIR threshold changes. As expected, if the SIR threshold γ increases, the multiplexing gain will go down for both f-FAMA and s-FAMA cases. Moreover, there is an SIR point after which the network multiplexing gain starts to drop considerably, as predicted by Corollary 4, i.e.,

$$\gamma > \begin{cases} \dfrac{MN\left(1-\frac{1}{\pi W}\right)}{U(U-1)} & \text{if } f\text{-FAMA}, \\ \left(\dfrac{MN}{U}\right)^{\frac{1}{U-1}}\left(1-\dfrac{1}{\pi W}\right) & \text{if } s\text{-FAMA}. \end{cases} \quad (52)$$

For example, in the f-FAMA case, when $M = 70$, $U = 50$, $N = 500$ and $W = 2$, it can be found from (52) that $\gamma = 10.8$dB is the breaking point where the multiplexing gain begins to substantially fall, which agrees very much with the results in Fig. 5(a)(ii). Similar but less accurate results can be seen for the s-FAMA case. For example, if $M = 5$, $U = 4$, $N = 100$ and $W = 5$, then (52) estimates that $\gamma = 6.7$dB will be the breaking point, which appears to be slightly larger than what is observed in Fig. 5(b)(ii).

Finally, the results in Figs. 5(a)(iii) & (b)(iii) examine the change of multiplexing gain, m, against the size of the fluid antenna at each UE, W. By changing the subject of (38) in Corollary 4, it can easily be shown that if

$$W > \begin{cases} \dfrac{1}{\pi\left(1-\frac{\gamma U(U-1)}{MN}\right)} & \text{if } f\text{-FAMA}, \\ \dfrac{1}{\pi\left[1-\gamma\left(\frac{U}{MN}\right)^{\frac{1}{U-1}}\right]} & \text{if } s\text{-FAMA}, \end{cases} \quad (53)$$

then $m \approx U$. Again, for the f-FAMA system, (53) is really accurate. When $M = 90$, $U = 50$, $\gamma = 10$dB and $N = 500$, (53) estimates that $W = 0.7$ is the point at which $m \approx U$, which agrees with the results in the figure.

VI. Conclusion

This paper attempted to combine opportunistic scheduling and FAMA for improved multiple access performance, where opportunism has helped alleviate greatly the burden of fluid antenna at each UE. Our objective was to quantify the benefits of the synergy between opportunistic scheduling and FAMA by analyzing the multiplexing gain of the network. This was

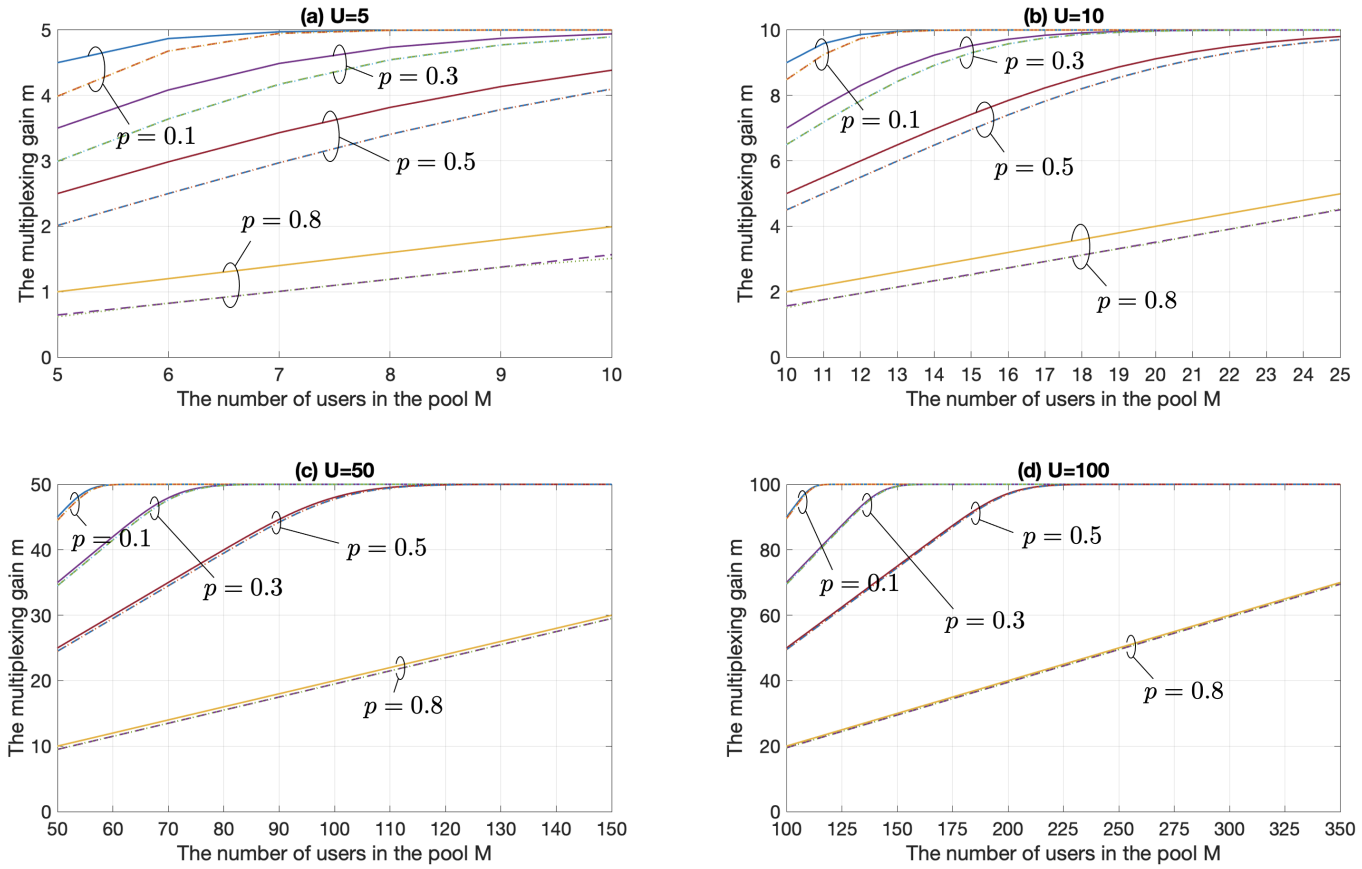

Fig. 3. The multiplexing gain results against the number of users in the selection pool for different number of selected users, U and outage probability achieved by the fluid antenna at each selected UE if (a) $U = 5$, (b) $U = 10$, (c) $U = 50$ and (d) $U = 100$. When $U = M$, no opportunistic scheduling is used. The solid lines refer to the exact results (21a) while the dashed lines are for the approximations (33) and the dotted lines correspond to the expression (44). Note that in the figures, the dashed and dotted lines overlap, meaning that the approximation of (44) to (33) is very accurate.

achieved by deriving various bounds and approximations on the multiplexing gain, which then facilitated the unpacking of the performance against key system parameters such as the number of UEs in the selection pool (M), the number of UEs selected to communicate on the same time-frequency channel (U) and the interference immunity at each fluid antenna (p). Both f-FAMA and s-FAMA systems were considered, with f-FAMA being the more powerful but less practical version than s-FAMA. Our analysis uncovered the rate of increase of the multiplexing gain w.r.t. M, from which we came up with a condition of the system parameters where the opportunistic FAMA network approached the maximum multiplexing gain $m \approx U$. Numerical results were provided and discussed to gain useful insights of the operation of the opportunistic FAMA networks and the capability of the synergy was revealed.

APPENDICES

A. *Proof of Theorem 3*

To begin with, we rearrange (21d) to get

$$\operatorname{erfc}\left(\frac{(1-p)M-U}{\sqrt{2Mp(1-p)}}\right) \geq 2\left(1-\frac{m}{U}\right). \tag{54}$$

Now, consider the situation $0 \leq m \leq \frac{U}{2}$, which implies that $1 \leq 2\left(1-\frac{m}{U}\right) \leq 2$ and $\alpha \leq 0$. Thus, we can rewrite (54) as

$$\frac{(1-p)M-U}{\sqrt{2Mp(1-p)}} \leq \alpha = -|\alpha| \leq 0, \tag{55}$$

which further implies that

$$(1-p)M - U \leq 0 \Rightarrow M \leq \frac{U}{1-p}. \tag{56}$$

It should be noted that in (55), the original inequality in (54) is flipped because $\operatorname{erfc}(\cdot)$ is a decreasing function. Squaring (55) on both sides (and flipping the inequality again because both sides are negative), we obtain

$$f(M) = M^2 - \left(\frac{2}{1-p}\right)(U+\alpha^2 p)M + \left(\frac{U}{1-p}\right)^2 \geq 0. \tag{57}$$

The roots of $f(M) = 0$ can be easily found as

$$M = \frac{U+\alpha^2 p}{1-p} \pm \frac{\sqrt{(\alpha^2 p)(\alpha^2 p + 2U)}}{1-p}. \tag{58}$$

Denoting the smaller root as M_1 and the larger root as M_2, (57) requires that $M \leq M_1$ or $M \geq M_2$. We can see that

$$M_1 = \frac{U+\alpha^2 p}{1-p} - \frac{\sqrt{(\alpha^2 p)(\alpha^2 p + 2U)}}{1-p} < \frac{U}{1-p} \tag{59}$$

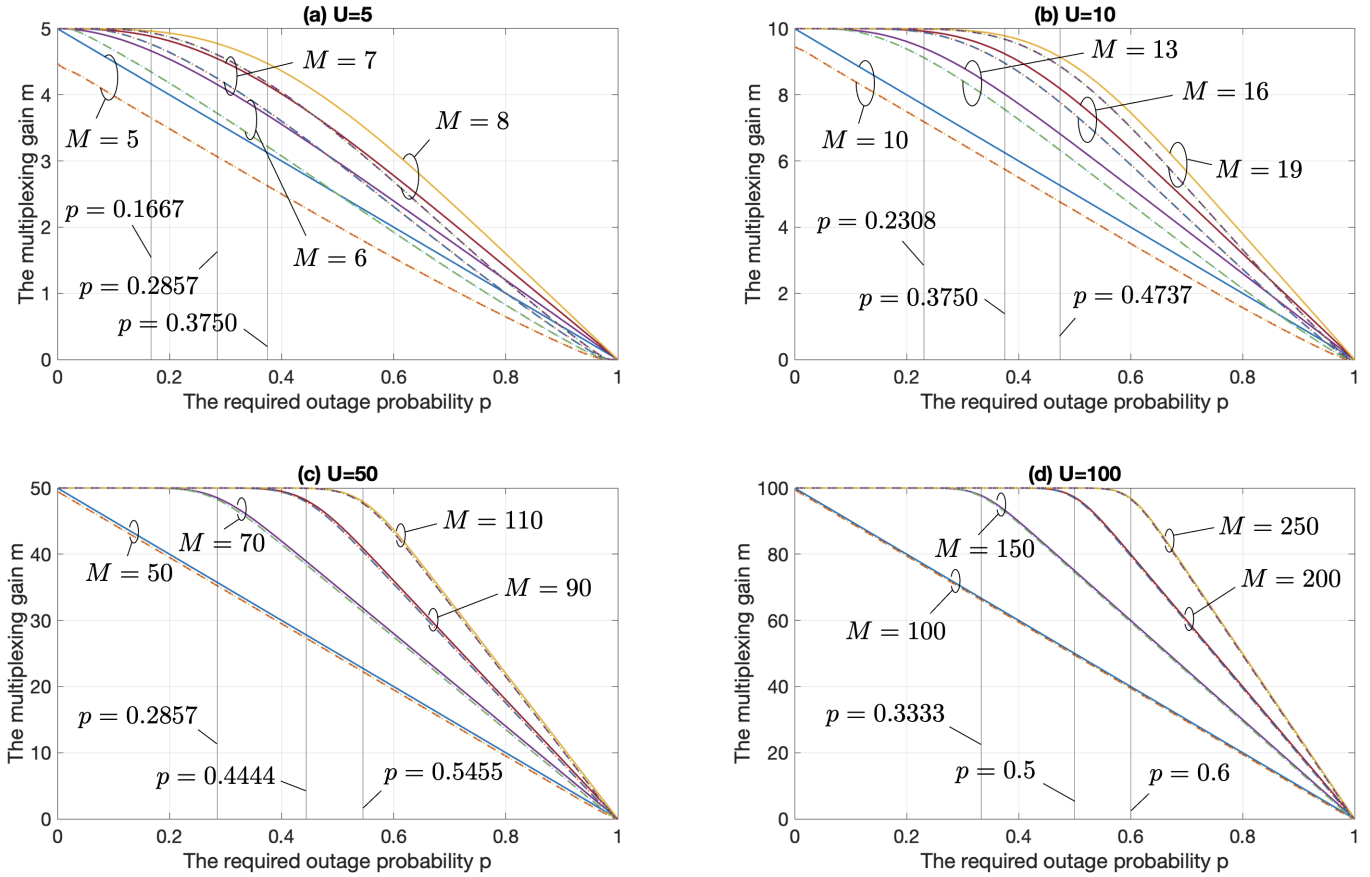

Fig. 4. The multiplexing gain results against the outage probability for the fluid antenna at each UE for different numbers of users, U and M. When $U = M$, again, no opportunistic scheduling is used. As before, the solid lines refer to the exact results (21a) while the dashed lines are for the approximations (33) and the dotted lines correspond to the expression (44). The approximation of (44) to (33) is again very accurate.

and

$$M_2 = \frac{U+\alpha^2 p}{1-p} + \frac{\sqrt{(\alpha^2 p)(\alpha^2 p+2U)}}{1-p} > \frac{U}{1-p}. \quad (60)$$

Combining (59) and (60) with (56), we then obtain $M \leq M_1$ which proves the result in (23).

Now, we proceed with the case $\frac{U}{2} \leq m \leq U$. In this case, $0 \leq 2\left(1-\frac{m}{U}\right) \leq 1$. Note that (55) is still true except that $\alpha \geq 0$. We also note that when $m = \frac{U}{2}$ we have $\alpha = 0$ and (23) is reduced to (56). Therefore, for $m \geq \frac{U}{2}$, we are interested in the case $M \geq \frac{U}{1-p}$. Hence, (55) yields

$$f(M) = M^2 - \left(\frac{2}{1-p}\right)(U+\alpha^2 p)M + \left(\frac{U}{1-p}\right)^2 \leq 0, \quad (61)$$

which gives the solution $\frac{U}{1-p} \leq M \leq M_2$, which arrives the condition (24) and therefore the proof is completed.

B. Proof of Theorem 4

If $0.0786U \leq m \leq \frac{U}{2}$, then it is easy to see that $-1 < \alpha \leq 0$. Then we have $\alpha^2 p \leq 1$. Using (23), we get

$$M \leq \frac{U+\alpha^2 p - \sqrt{(\alpha^2 p)(\alpha^2 p+2U)}}{1-p} \overset{(a)}{\lesssim} \frac{U-\sqrt{2\alpha^2 pU}}{1-p} = \frac{U-|\alpha|\sqrt{2U}\sqrt{p}}{1-p}, \quad (62)$$

where (a) uses the fact that $U \gg \alpha^2 p$. Simplifying (62) gives

$$g_1(p) = p - \frac{|\alpha|\sqrt{2U}}{M}\sqrt{p} - \left(1-\frac{U}{M}\right) \geq 0. \quad (63)$$

The roots of $g_1(p) = 0$ are given by

$$\sqrt{p} = \frac{|\alpha|}{M}\sqrt{\frac{U}{2}} \pm \sqrt{\frac{\alpha^2}{M^2}\frac{U}{2} + 1 - \frac{U}{M}}. \quad (64)$$

Denoting the smaller root as $\sqrt{p_1}$ and the larger root as $\sqrt{p_2}$, we can easily see that $\sqrt{p_1} < 0$ which is impossible and thus rejected. As a result, $g_1(p) \geq 0$ gives the solution $\sqrt{p} \geq \sqrt{p_2}$. For large M, we can simplify

$$\sqrt{\frac{\alpha^2}{M^2}\frac{U}{2} + 1 - \frac{U}{M}} = \sqrt{1 - \frac{U}{M}\left(1-\frac{\alpha^2}{2M}\right)} \overset{(a)}{\approx} \sqrt{1-\frac{U}{M}} \overset{(b)}{\approx} 1 - \frac{U}{2M}, \quad (65)$$

where (a) uses $M \gg \alpha^2$ and (b) is due to $U < M$. Therefore, we have the lower bound

$$\sqrt{p} \geq 1 - \left(\frac{U}{2M} - \frac{|\alpha|}{M}\sqrt{\frac{U}{2}}\right). \quad (66)$$

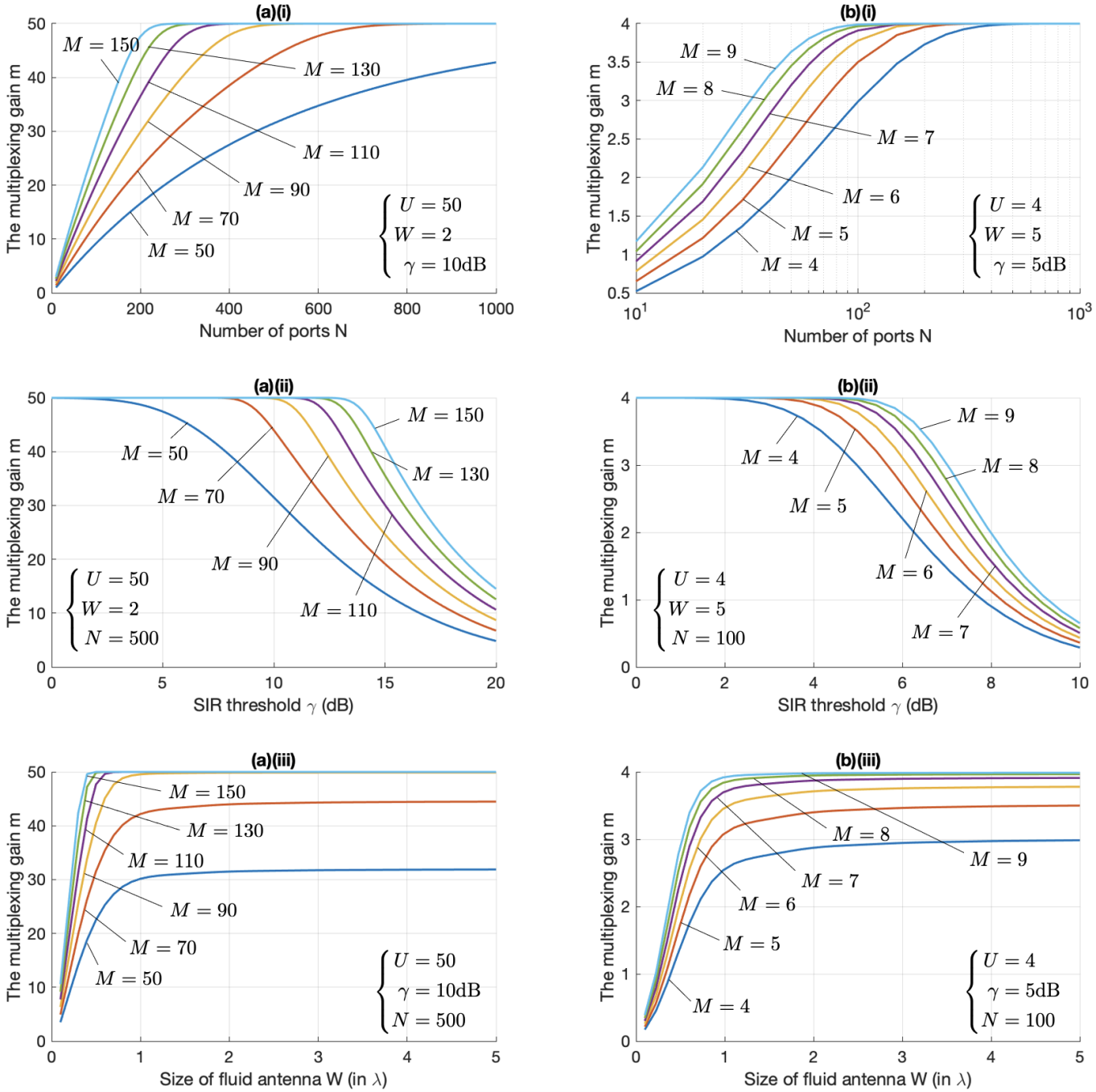

Fig. 5. The multiplexing gain results of the opportunistic (a) f-FAMA and (b) s-FAMA networks against various different parameters such as (i) the number of ports, (ii) the SIR threshold and (iii) the size of fluid antenna at each UE. In the figures, only exact results (21a) using (9) and (10) are provided.

Squaring both sides of the above, employing the approximation $(1-x)^2 \approx 1-2x$ for small x and noting that $|\alpha| = -\alpha$ in this case, we obtain the result (26).

Now, consider the case $\frac{U}{2} \leq m < 0.9214U$. In this case, $0 \leq \alpha < 1$ and $\alpha = |\alpha|$. Again, we have $\alpha^2 p < 1 \ll U$. Using (24), we can get

$$M \leq \frac{U + \alpha^2 p + \sqrt{(\alpha^2 p)(\alpha^2 p + 2U)}}{1-p} \lesssim \frac{U + |\alpha|\sqrt{2U}\sqrt{p}}{1-p}, \tag{67}$$

which can be rewritten as

$$g_2(p) = p + \frac{|\alpha|\sqrt{2U}}{M}\sqrt{p} - \left(1 - \frac{U}{M}\right) \geq 0. \tag{68}$$

Finding the two roots of $g_2(p) = 0$ and noting that the small root should be rejected, we then obtain

$$\sqrt{p} \geq 1 - \left(\frac{U}{2M} + \frac{|\alpha|}{M}\sqrt{\frac{U}{2}}\right). \tag{69}$$

Finally, squaring both sides, utilizing the approximation $(1-x)^2 \approx 1-2x$ for small x and knowing that $|\alpha| = \alpha$, we again

derive the result (26), which completes the proof.

C. Proof of Theorem 9

First, we recognize a tight approximation [49, (6)]

$$\operatorname{erfc}(x) \approx \frac{\left(1-e^{-Ax}\right)e^{-x^2}}{B\sqrt{\pi}x}, \text{ for } x \geq 0, \tag{70}$$

where $A \doteq 1.98$ and $B \doteq 1.135$. Note that when $x = 0$, the right hand side is $\frac{A}{B\sqrt{\pi}} \approx 1$. When $(1-p)M \geq U$, the input argument to $\operatorname{erfc}(\cdot)$ of each term inside the summation in (33) is always positive. Then we can apply (70) to (33) so that

$$m \approx U - \frac{1}{B}\sqrt{\frac{Mp(1-p)}{2\pi}} \times \sum_{u=1}^{U} \frac{\left(1-e^{-\frac{A[(1-p)M-u]}{\sqrt{2Mp(1-p)}}}\right) e^{-\frac{[(1-p)M-u]^2}{2Mp(1-p)}}}{(1-p)M-u}, \tag{71}$$

which is the same as (44).

Now, for the case $(1-p)M < U$ and $u = \{1, \ldots, U\}$, we know that $(1-p)M - u$ can be positive or negative. By the definition of (45), U_0 is the number at which $(1-p)M - u$ switches its sign when $u = U_0$ changes to $u = U_0 + 1$. Thus, some of the terms inside the summation are positive and some negative. Hence, we split the summation into two sums, one for $u \leq U_0$ and another $u \geq U_0 + 1$. As such, we have (72) (see top of next page) in which (a) splits the summation, (b) uses the identity $\operatorname{erfc}(-x) = 2 - \operatorname{erfc}(x)$, (c) is obtained after some simplifications, and (d) adopts the approximation (70). After some manipulations, (72) is expressed as (44).

D. Proof of Theorem 10

From Corollary 3, it is known that when $p < 1 - \frac{U}{M}$ (i.e., $M > \frac{U}{1-p}$), $m \approx U$. On the other hand, it is obvious that if $p = 1$, then $m = 0$. Also, the multiplexing gain is a decreasing function of p. Thus, it is possible to approximate m by a linear function of p for $p > 1 - \frac{U}{M}$, which suggests immediately that $m = M(1-p)$. However, instead of simply accepting this approximation, we here aim to show that

$$\frac{\partial m}{\partial p} \approx -M \tag{73}$$

for most part of $1 - \frac{U}{M} < p \leq 1$, which then implies that the approximation is very accurate.

We begin the proof by obtaining the derivative of (33) as

$$\frac{\partial m}{\partial p} = -\frac{1}{2\sqrt{2\pi M}} \times \sum_{u=1}^{U} \frac{(1-p)M + (2p-1)u}{[p(1-p)]^{1.5}} e^{-\frac{[(1-p)M-u]^2}{2Mp(1-p)}} \tag{74}$$

and evaluate the derivative when $p = 1 - \frac{U}{2M}$ is the mid-point in the interval $[1 - \frac{U}{M}, 1)$, which gives (75) (see next page), where (a) is the result of direct substitution $p = 1 - \frac{U}{2M}$, (b) uses the approximations $1 - \frac{U}{M} \approx 1$ and $1 - \frac{U}{2M} \approx 1$, and (c) separates it into two sums A and B.

Before we proceed, we find the following integral useful:

$$\int_{-\infty}^{\infty} e^{-t^2} dt = \sqrt{\pi}, \tag{76}$$

which can be shown by recognizing the total probability of a standard Gaussian random variable $\frac{1}{\sqrt{2\pi}} \int_{-\infty}^{\infty} e^{-\frac{x^2}{2}} dx = 1$.

Now, A can be derived as

$$A \overset{(a)}{=} \frac{1}{2} \sum_{k=-\frac{U}{2}}^{\frac{U}{2}-1} e^{-\frac{k^2}{U}} \frac{1}{\sqrt{U}} \overset{(b)}{\approx} \frac{1}{2} \int_{-\infty}^{\infty} e^{-x^2} dx = \frac{\sqrt{\pi}}{2}, \tag{77}$$

where (a) applies the change of variables $k = \frac{U}{2} - u$ and (b) treats $\frac{1}{\sqrt{U}} = dx$ and $x = \frac{k}{\sqrt{U}}$ for large U and then uses (76) to obtain the final result. Similarly, we can obtain B by

$$\begin{aligned} B &\overset{(a)}{=} \frac{1}{\sqrt{U}} \sum_{k=-\frac{U}{2}}^{\frac{U}{2}-1} \frac{\frac{U}{2}-k}{U} e^{-\frac{k^2}{U}} \\ &\overset{(b)}{=} \frac{1}{2} \sum_{k=-\frac{U}{2}}^{\frac{U}{2}-1} e^{-\frac{k^2}{U}} \frac{1}{\sqrt{U}} - \frac{1}{\sqrt{U}} \sum_{k=-\frac{U}{2}}^{\frac{U}{2}-1} \frac{k}{\sqrt{U}} e^{-\frac{k^2}{U}} \frac{1}{\sqrt{U}} \\ &\overset{(c)}{\approx} \frac{1}{2} \int_{-\infty}^{\infty} e^{-x^2} dx - 0 \times \int_{-\infty}^{\infty} x e^{-x^2} dx \overset{(d)}{=} \frac{\sqrt{\pi}}{2}, \end{aligned} \tag{78}$$

where (a) uses the substitution $k = \frac{U}{2} - u$, (b) splits the sum into two parts, (c) approximates the sums using integration when U is large and finally applies (76) to get the result. As a consequence, the derivative can be found as

$$\frac{\partial m}{\partial p} = -\frac{M}{\sqrt{\pi}} \left(\frac{\sqrt{\pi}}{2} + \frac{\sqrt{\pi}}{2} \right) = -M. \tag{79}$$

Finally, the above analysis can be repeated if $p = 1 - \frac{U}{2M} \pm \delta$ when $\delta < \frac{U}{2M}$ is small, which completes the proof.

REFERENCES

[1] X. Lu, P. Wang, D. Niyato, D. I. Kim and Z. Han, "Wireless networks with RF energy harvesting: A contemporary survey," *IEEE Commun. Surveys & Tutorials*, vol. 17, no. 2, pp. 757–789, 2015.

[2] A. Mukherjee, S. A. A. Fakoorian, J. Huang and A. L. Swindlehurst, "Principles of physical layer security in multiuser wireless networks: A survey," *IEEE Commun. Surveys & Tutorials*, vol. 16, no. 3, pp. 1550–1573, 2014.

[3] W. Shi, J. Cao, Q. Zhang, Y. Li and L. Xu, "Edge computing: Vision and challenges," *IEEE Internet of Things J.*, vol. 3, no. 5, pp. 637–646, Oct. 2016.

[4] M. A. Alsheikh, S. Lin, D. Niyato and H. Tan, "Machine learning in wireless sensor networks: Algorithms, strategies, and applications," *IEEE Commun. Surveys & Tutorials*, vol. 16, no. 4, pp. 1996–2018, 2014.

[5] C. Jiang, H. Zhang, Y. Ren, Z. Han, K.-C. Chen and L. Hanzo, "Machine learning paradigms for next-generation wireless networks," *IEEE Wireless Commun.*, vol. 24, no. 2, pp. 98–105, Apr. 2017.

[6] C. Zhang, P. Patras and H. Haddadi, "Deep learning in mobile and wireless networking: A survey," *IEEE Commun. Surveys & Tutorials*, vol. 21, no. 3, pp. 2224–2287, 2019.

[7] F. Tang, Y. Kawamoto, N. Kato and J. Liu, "Future intelligent and secure vehicular network toward 6G: Machine-learning approaches," *Proc. IEEE*, vol. 108, no. 2, pp. 292–307, Feb. 2020.

[8] C. Bockelmann *et al.*, "Massive machine-type communications in 5G: Physical and MAC-layer solutions," *IEEE Commun. Mag.*, vol. 54, no. 9, pp. 59–65, Sep. 2016.

[9] F. Tariq, M. R. A. Khandaker, K. K. Wong, M. A. Imran, M. Bennis and M. Debbah, "A speculative study on 6G," *IEEE Wireless Commun.*, vol. 27, no. 4, pp. 118–125, Aug. 2020.

$$
\begin{aligned}
m &\overset{(a)}{=} U - \frac{1}{2}\left[\sum_{u=1}^{U_0}\operatorname{erfc}\left(\frac{(1-p)M-u}{\sqrt{2Mp(1-p)}}\right) + \sum_{u=U_0+1}^{U}\operatorname{erfc}\left(\frac{(1-p)M-u}{\sqrt{2Mp(1-p)}}\right)\right] \\
&\overset{(b)}{=} U - \frac{1}{2}\left\{\sum_{u=1}^{U_0}\operatorname{erfc}\left(\frac{(1-p)M-u}{\sqrt{2Mp(1-p)}}\right) + \sum_{u=U_0+1}^{U}\left[2-\operatorname{erfc}\left(\frac{u-(1-p)M}{\sqrt{2Mp(1-p)}}\right)\right]\right\} \\
&\overset{(c)}{=} U_0 - \frac{1}{2}\sum_{u=1}^{U_0}\operatorname{erfc}\left(\frac{(1-p)M-u}{\sqrt{2Mp(1-p)}}\right) + \frac{1}{2}\sum_{u=U_0+1}^{U}\operatorname{erfc}\left(\frac{u-(1-p)M}{\sqrt{2Mp(1-p)}}\right) \\
&\overset{(d)}{\approx} U_0 - \frac{1}{B}\sqrt{\frac{Mp(1-p)}{2\pi}}\sum_{u=1}^{U_0}\frac{\left(1-e^{-\frac{A[(1-p)M-u]}{\sqrt{2Mp(1-p)}}}\right)e^{-\frac{[(1-p)M-u]^2}{2Mp(1-p)}}}{(1-p)M-u} \\
&\qquad + \frac{1}{B}\sqrt{\frac{Mp(1-p)}{2\pi}}\sum_{u=U_0+1}^{U}\frac{\left(1-e^{\frac{A[(1-p)M-u]}{\sqrt{2Mp(1-p)}}}\right)e^{-\frac{[(1-p)M-u]^2}{2Mp(1-p)}}}{u-(1-p)M}
\end{aligned} \tag{72}
$$

$$
\begin{aligned}
\frac{\partial m}{\partial p} &\overset{(a)}{=} -\frac{1}{2\sqrt{2\pi M}\left[\left(1-\frac{U}{2M}\right)\frac{U}{2M}\right]^{1.5}}\sum_{u=1}^{U}\left[\frac{U}{2}+\left(1-\frac{U}{M}\right)u\right]e^{-\frac{\left(\frac{U}{2}-u\right)^2}{U\left(1-\frac{U}{2M}\right)}} \\
&\overset{(b)}{\approx} -\frac{M}{\sqrt{\pi}U^{1.5}}\sum_{u=1}^{U}\left(\frac{U}{2}+u\right)e^{-\frac{\left(\frac{U}{2}-u\right)^2}{U}} \\
&\overset{(c)}{=} -\frac{M}{\sqrt{\pi}}\left[\underbrace{\frac{1}{2\sqrt{U}}\sum_{u=1}^{U}e^{-\frac{\left(\frac{U}{2}-u\right)^2}{U}}}_{A} + \underbrace{\frac{1}{\sqrt{U}}\sum_{u=1}^{U}\frac{u}{U}e^{-\frac{\left(\frac{U}{2}-u\right)^2}{U}}}_{B}\right]
\end{aligned} \tag{75}
$$

[10] W. Saad, M. Bennis and M. Chen, "A vision of 6G wireless systems: Applications, trends, technologies, and open research problems," *IEEE Netw.*, vol. 34, no. 3, pp. 134–142, May/Jun. 2020.

[11] D. Gesbert, M. Kountouris, R. W. Heath, C. Chae and T. Salzer, "Shifting the MIMO paradigm," *IEEE Signal Proc. Mag.*, vol. 24, no. 5, pp. 36–46, Sep. 2007.

[12] E. G. Larsson, O. Edfors, F. Tufvesson and T. L. Marzetta, "Massive MIMO for next generation wireless systems," *IEEE Commun. Mag.*, vol. 52, no. 2, pp. 186–195, Feb. 2014.

[13] Y. Saito, Y. Kishiyama, A. Benjebbour, T. Nakamura, A. Li and K. Higuchi, "Non-orthogonal multiple access (NOMA) for cellular future radio access," in *Proc. IEEE Veh. Technol. Conf. (VTC Spring)*, pp. 1–5, 2-5 Jun. 2013, Dresden, Germany.

[14] L. Dai, B. Wang, Y. Yuan, S. Han, I. Chih-lin and Z. Wang, "Non-orthogonal multiple access for 5G: Solutions, challenges, opportunities, and future research trends," *IEEE Commun. Mag.*, vol. 53, no. 9, pp. 74–81, Sep. 2015.

[15] K. K. Wong, K. F. Tong, Y. Shen, Y. Chen, and Y. Zhang, "Bruce Lee-inspired fluid antenna system: Six research topics and the potentials for 6G," *Frontiers in Commun. and Netw., section Wireless Commun.*, 3:853416, Mar. 2022.

[16] K. K. Wong, and K. F. Tong, "Fluid antenna multiple access," *IEEE Trans. Wireless Commun.*, vol. 21, no. 7, pp. 4801–4815, Jul. 2022.

[17] K. K. Wong, K. F. Tong, Y. Chen, and Y. Zhang, "Fast fluid antenna multiple access enabling massive connectivity," *IEEE Commun. Letters*, vol. 27, no. 2, pp. 711–715, Feb. 2023.

[18] K. K. Wong, D. Morales-Jimenez, K. F. Tong, and C. B. Chae, "Slow fluid antenna multiple access," to appear *IEEE Trans. Commun.*, 2023.

[19] N. Waqar, K. K. Wong, K. F. Tong, A. Sharples, and Y. Zhang, "Deep learning enabled slow fluid antenna multiple access," to appear in *IEEE Commun. Letters*, 2023.

[20] K. K. Wong, K. F. Tong, Y. Chen, and Y. Zhang, "Extra-large MIMO enabling slow fluid antenna massive access for millimeter-wave bands," *IET Elect. Letters*, vol. 58, no. 25, pp. 1016–1018, Dec. 2022.

[21] K. N. Paracha, A. D. Butt, A. S. Alghamdi, S. A. Babale, and P. J. Soh, "Liquid metal antennas: Materials, fabrication and applications," *Sensors 2020*, 20, 177.

[22] Y. Huang, L. Xing, C. Song, S. Wang and F. Elhouni, "Liquid antennas: Past, present and future," *IEEE Open J. Antennas and Propag.*, vol. 2, pp. 473–487, 2021.

[23] B. A. Cetiner, H. Jafarkhani, Jiang-Yuan Qian, Hui Jae Yoo, A. Grau and F. De Flaviis, "Multifunctional reconfigurable MEMS integrated antennas for adaptive MIMO systems," *IEEE Commun. Mag.*, vol. 42, no. 12, pp. 62–70, Dec. 2004.

[24] A. Grau Besoli and F. De Flaviis, "A multifunctional reconfigurable pixeled antenna using MEMS technology on printed circuit board," *IEEE Trans. Antennas & Propag.*, vol. 59, no. 12, pp. 4413–4424, Dec. 2011.

[25] S. Song and R. D. Murch, "An efficient approach for optimizing frequency reconfigurable pixel antennas using genetic algorithms," *IEEE Trans. Antennas & Propag.*, vol. 62, no. 2, pp. 609–620, Feb. 2014.

[26] X. Yan, L. Li, H. C. Zhang and J. Y. Han, "Broadband polarization-reconfigurable liquid dielectric resonator antenna controlled by gravity," *IEEE Antennas & Wireless Propag. Letters*, vol. 21, no. 10, pp. 2105–2109, Oct. 2022.

[27] T. Zhang, Y. Chen and S. Yang, "A wideband frequency- and polarization-reconfigurable liquid metal-based spiral antenna," *IEEE Antennas & Wireless Propag. Letters*, vol. 21, no. 7, pp. 1477–1481, Jul. 2022.

[28] X. Geng *et al.*, "Pattern-reconfigurable liquid metal magneto-electric dipole antenna," *IEEE Antennas & Wireless Propag. Letters*, vol. 21, no. 8, pp. 1683–1687, Aug. 2022.

[29] Y. Zhou, G. Zhao, X. Yu Li and M. S. Tong, "A liquid-metal-based crossed-slot antenna with polarization and continuous-frequency reconfiguration," *IEEE Open J. Antennas & Propag.*, vol. 3, pp. 1102–1108, 2022.

[30] L. Li, X. Yan, H. C. Zhang and Q. Wang, "Polarization- and frequency-reconfigurable patch antenna using gravity-controlled liquid metal," *IEEE*

Trans. Circuits & Syst. II: Express Briefs, vol. 69, no. 3, pp. 1029–1033, Mar. 2022.
[31] Y. Shen, K. F. Tong, and K. K. Wong, "Reconfigurable surface wave fluid antenna for spatial MIMO applications," in *Proc. Int. Conf. Electromag. Adv. Appl. (ICEAA 2021)*, 9-13 Aug. 2021, Honolulu, Hawaii, USA.
[32] H. Wang, Y. Shen, K. F. Tong, and K. K. Wong, "Continuous electrowetting surface-wave fluid antenna for mobile communications," in Proc. *IEEE Technol., Education and Netw. Conf. (TENCON 2022)*, 1-4 Nov. 2022, Hong Kong SAR, China.
[33] J. O. Martínez *et al.*, "Toward liquid reconfigurable antenna arrays for wireless communications," *IEEE Commun. Mag.*, vol. 60, no. 12, pp. 145–151, Dec. 2022.
[34] M. Khammassi, A. Kammoun, and M.-S. Alouini, "A new analytical approximation of the fluid antenna system channel," [Online] arXiv preprint arXiv:2203.09318, 2022.
[35] C. Psomas, G. M. Kraidy, K. K. Wong, and I. Krikidis, "On the diversity and coded modulation design of fluid antenna systems," [Online] arXiv preprint arXiv:2205.01962, 2022.
[36] P. Mukherjee, C. Psomas, and I. Krikidis, "On the level crossing rate of fluid antenna systems," [Online] arXiv preprint arXiv:2205.01711, 2022.
[37] L. Tlebaldiyeva, G. Nauryzbayev, S. Arzykulov, A. Eltawil, and T. Tsiftsis, "Enhancing QoS through fluid antenna systems over correlated Nakagami-m fading channels," in Proc. *IEEE Wireless Commun. & Netw. Conf. (WCNC)*, pp. 78–83, 10-13 Apr. 2022, Austin, TX, USA.
[38] C. Skouroumounis and I. Krikidis, "Fluid antenna with linear MMSE channel estimation for large-scale cellular networks," *IEEE Trans. Commun.*, vol. 71, no. 2, pp. 1112–1125, Feb. 2023.
[39] L. Zhu, W. Ma, and R. Zhang, "Modeling and performance analysis for movable antenna enabled wireless communications," [Online] arXiv preprint arXiv:2210.05325, 2022.
[40] W. Ma, L. Zhu, and R. Zhang, "MIMO capacity characterization for movable antenna systems," [Online] arXiv preprint arXiv:2210.05396, 2022.
[41] Z. Chai, K. K. Wong, K. F. Tong, Y. Chen, and Y. Zhang, "Port selection for fluid antenna systems," *IEEE Commun. Letters*, vol. 26, no. 5, pp. 1180–1184, May 2022.
[42] A. Asadi, and V. Mancuso, "A survey on opportunistic scheduling in wireless communications," *IEEE Commun. Surveys & Tutorials*, vol. 15, no. 4, pp. 1671–1688, 2013.
[43] P. Viswanath, D. N. C. Tse, and R. Laroia, "Opportunistic beamforming using dumb antennas," *IEEE Trans. Inform. Theory*, vol. 48, no. 6, pp. 1277–1294, Jun. 2002.
[44] K. K. Wong, K. F. Tong, Y. Chen and Y. Zhang, "Closed-form expressions for spatial correlation parameters for performance analysis of fluid antenna systems," *IET Elect. Letters*, vol. 58, no. 11, pp. 454–457, Apr. 2022
[45] K. K. Wong, K. F. Tong, Y. Chen and Y. Zhang, "Maximizing the network outage rate for fast fluid antenna multiple access systems," to appear *IET Commun.*, 2023.
[46] L. Ping, L. Liu, K. Wu, and W. K. Leung, "Interleave division multiple-access," *IEEE Trans. Wireless Commun.*, vol. 5, no. 4, pp. 938–947, Apr. 2006.
[47] K. S. Gilhousen *et al.*, "On the capacity of a cellular CDMA system," *IEEE Trans. Veh. Technol.*, vol. 40, no. 2, pp. 303–312, May 1991.
[48] J. Pitman, *Probability: Springer Texts in Statistics*, New York, Berlin, and Heidelberg: Springer, 1993.
[49] G. K. Karagiannidis and A. S. Lioumpas, "An improved approximation for the Gaussian Q-function," *IEEE Commun. Letters*, vol. 11, no. 8, pp. 644–646, Aug. 2007.

(Kit) Kai-Kit Wong (M'01-SM'08-F'16) received the BEng, the MPhil, and the PhD degrees, all in Electrical and Electronic Engineering, from the Hong Kong University of Science and Technology, Hong Kong, in 1996, 1998, and 2001, respectively. After graduation, he took up academic and research positions at the University of Hong Kong, Lucent Technologies, Bell-Labs, Holmdel, the Smart Antennas Research Group of Stanford University, and the University of Hull, UK. He is Chair in Wireless Communications at the Department of Electronic and Electrical Engineering, University College London, UK.

His current research centers around 5G and beyond mobile communications. He is a co-recipient of the 2013 IEEE Signal Processing Letters Best Paper Award and the 2000 IEEE VTS Japan Chapter Award at the IEEE Vehicular Technology Conference in Japan in 2000, and a few other international best paper awards. He is Fellow of IEEE and IET and is also on the editorial board of several international journals. He is the Editor-in-Chief for IEEE Wireless Communications Letters since 2020.

Kin Fai Tong (M'99-SM'13-F'23) received the B.Eng. and Ph.D. degrees in electronic engineering from the City University of Hong Kong in 1993 and 1997, respectively. After graduation, Dr. Tong worked in the Department of Electronic Engineering at City University of Hong Kong as a Research Fellow. Two years later, he took up the post Expert researcher in the Photonic Information Technology Group and Millimetre-wave Devices Group at the National Institute of Information and Communications Technology (NiCT), Japan, where his main research focused on photonic-millimeter-wave planar antennas at 10GHz, 38 GHz and 60 GHz for high-speed wireless communications systems. In 2005, he started his academic career in the Department of Electronic and Electrical Engineering, UCL, as a lecturer. Now Dr. Tong is Chair in Antennas, Microwave and Millimeter-wave Engineering in the department. His current research interests include millimeter-wave and THz antennas, fluid antennas, 3D printed antennas and sub-GHz long range IoT networks. He served as the General Co-Chair of the 2017 International Workshop on Electromagnetics (iWEM), and Lead Guest Editor of IEEE OJAP in 2020.

Yu Chen received the B.Eng. degree in electronic science and technology from the Beijing University of Posts and Telecommunications (BUPT), Beijing, China, in 2006, and the M.Sc. and the Ph.D. degrees from the Communications and Information Systems Group, University College London, London, U.K., in 2007 and 2013, respectively. Since 2015, he has been with the School of the Information and Communication Engineering, BUPT, Beijing, China, where he is currently a Lecturer. His general research interests include fluid antenna systems, end-to-end latency analysis and quality-of-service provisioning algorithm design, and cross-layer energy efficiency analysis.

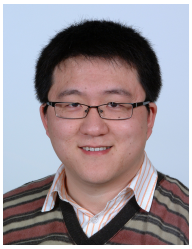

Yangyang Zhang received the B.S. and M.S. degrees in electronics and information engineering from Northeastern University, Shenyang, China, in 2002 and 2004 respectively, and the Ph.D. degree in electrical engineering from the University of Oxford,Oxford, U.K., in 2008.

He is currently taking the position of Executive Director of Kuang-Chi Science Limited, Hong Kong. His research interests include multiple-input multiple-output wireless communications and stochastic optimization algorithms. Dr. Zhang has been awarded more than 20 honors. Besides, he also authored and co-authored more than 40 refereed papers.

Chan-Byoung Chae (Fellow, IEEE) received the Ph.D. degree in electrical and computer engineering from The University of Texas at Austin (UT) in 2008.

Prior to joining UT, he was a Research Engineer at the Telecommunications Research and Development Center, Samsung Electronics, Suwon, South Korea, from 2001 to 2005. He is currently an Underwood Distinguished Professor with the School of Integrated Technology, Yonsei University, South Korea. Before joining Yonsei University, he was with Bell Labs, Alcatel-Lucent, Murray Hill, NJ, USA, from 2009 to 2011, as a Member of Technical Staff, and Harvard University, Cambridge, MA, USA, from 2008 to 2009, as a Post-Doctoral Research Fellow.

Dr. Chae was a recipient/co-recipient of the CES Innovation Award in 2023, the IEEE ICC Best Demo Award in 2022, the IEEE WCNC Best Demo Award in 2020, the Best Young Engineer Award from the National Academy of Engineering of Korea (NAEK) in 2019, the IEEE DySPAN Best Demo Award in 2018, the IEEE/KICS Journal of Communications and Networks Best Paper Award in 2018, the IEEE INFOCOM Best Demo Award in 2015, the IEIE/IEEE Joint Award for Young IT Engineer of the Year in 2014, the KICS Haedong Young Scholar Award in 2013, the *IEEE Signal Processing Magazine* Best Paper Award in 2013, the IEEE ComSoc AP Outstanding Young Researcher Award in 2012, and the IEEE VTS Dan. E. Noble Fellowship Award in 2008. He is currently the Editor-in-Chief of the IEEE TRANSACTIONS ON MOLECULAR, BIOLOGICAL, AND MULTI-SCALE COMMUNICATIONS and a Senior Editor of the IEEE WIRELESS COMMUNICATIONS LETTERS. He has served/serves as an Editor for the *IEEE Communications Magazine* since 2016, the IEEE TRANSACTIONS ON WIRELESS COMMUNICATIONS from 2012 to 2017, and the IEEE WIRELESS COMMUNICATIONS LETTERS since 2016. He is an IEEE ComSoc Distinguished Lecturer from 2020 to 2023. He is an IEEE Fellow and NAEK Fellow.